Research Square

Preprints are preliminary reports that have not undergone peer review.
They should not be considered conclusive, used to inform clinical practice,
or referenced by the media as validated information.

Targeting SERPINE1 suppresses cGAS-STING-mediated fibroblast senescence and attenuates intestinal inflammation in Crohn's disease

Pule Liu
Zhongnan Hospital of Wuhan University
Ruidong Wang
Zhongnan Hospital of Wuhan University
Yali Yu
Zhongnan Hospital of Wuhan University
Yumei Ning
Zhongnan Hospital of Wuhan University
Minhu Chen
First Affiliated Hospital of Sun Yat-sen University
Mei Ye
wumeiye08@163.com

Zhongnan Hospital of Wuhan University

Research Article

Keywords: Crohn's disease, Fibroblast, Cellular senescence, SERPINE1, Single-cell RNA sequencing, Microenvironment remodeling, cGAS-STING

Posted Date: June 5th, 2026

DOI: https://doi.org/10.21203/rs.3.rs-9810404/v1

License: This work is licensed under a Creative Commons Attribution 4.0 International License.
Read Full License

Additional Declarations: No competing interests reported.

Abstract

Background

Cellular senescence and the senescence-associated secretory phenotype (SASP) are recognized drivers of chronic inflammation. This study aims to characterize a specific senescent fibroblast subset and its role in reshaping the immune landscape of Crohn's disease (CD).

Methods

Single-cell and bulk transcriptomic data from CD patients were analyzed to identify senescent cell populations and map intercellular communication networks. Mechanistic and functional validations were conducted utilizing macrophage-fibroblast co-culture systems and a dextran sulfate sodium (DSS)-induced colitis mouse model treated with the selective SERPINE1 inhibitor, TM5441.

Results

Transcriptomic profiling identified a localized, previously uncharacterized subpopulation of SERPINE1$^+$ fibroblasts in inflamed CD tissues that exhibited high senescence scores, G1 cell-cycle arrest, and a pro-inflammatory secretory profile. Interaction analyses revealed that IL1RN$^+$ macrophages induce this fibroblast senescence primarily via paracrine TNF-α signaling. Mechanistically, SERPINE1 sustains this senescent phenotype by promoting the activation of the cGAS-STING pathway. Importantly, targeted pharmacological inhibition of SERPINE1 using TM5441 significantly attenuated DSS-induced colitis and effectively suppressed cGAS-STING-mediated cellular senescence in vivo.

Conclusion

SERPINE1 acts as a central driver of pathogenic fibroblast senescence in the CD mucosal microenvironment by activating the cGAS-STING pathway. Consequently, pharmacological inhibition of SERPINE1 presents a promising therapeutic strategy for managing intestinal inflammation in Crohn's disease.

Background

Crohn's disease (CD) is a chronic inflammatory bowel disease of unknown etiology, with contributions from genetic, environmental, and microbial factors(1). The immune environment in the gut shows high heterogeneity(2, 3), wherein stromal and immune cells, together with their secreted cytokines, drive disease pathogenesis and represent therapeutic targets(4, 5). Although biologic therapies such as anti-TNF agents (e.g., infliximab) have transformed disease management, a significant proportion of patients

either fail to respond or lose response over time(6, 7). Therefore, we need alternative therapies that target the disease mechanism.

Cellular senescence is a stable cell cycle arrest triggered by stress(8). A hallmark of senescent cells is the upregulation of cyclin-dependent kinase inhibitors, notably p21 and p16, which enforce cell cycle exit(9, 10). Notably, p16 and p21 have been identified as senescence markers in patients with IBD, suggesting their potential association with disease progression and mucosal inflammation(11). Senescent cells remain metabolically active(12, 13) and secrete a repertoire of pro-inflammatory factors, collectively termed the senescence-associated secretory phenotype (SASP) (14). This sustained SASP generates a chronic inflammatory milieu that drives tissue dysfunction and disease progression(15).

Plasminogen activator inhibitor-1 (PAI-1), encoded by SERPINE1, is a recognized component of the SASP(16–18). Beyond its role as a secreted marker, PAI-1 actively drives cellular senescence and organismal aging(17, 19, 20). PAI-1 is necessary and sufficient to induce senescence downstream of p53 and p21(20–22). Elevated SERPINE1 expression promotes tumor progression and modulates immune responses(23, 24), suggesting that SERPINE1 shapes the immune microenvironment. Given its emerging role as a key mediator of senescence(17, 20), SERPINE1 represents a candidate contributor to chronic inflammatory diseases. Nevertheless, its role in the intestinal microenvironment of CD has not been systematically investigated.

Accumulating evidence has established the cGAS-STING signaling pathway as a critical regulator of cellular senescence(25). Mechanistically, cGAS senses cytosolic DNA—often derived from mitochondrial damage or genomic instability—and initiates signaling cascades that enforce cell cycle arrest and drive the SASP(26, 27). The cGAS-STING pathway has also been implicated in the pathogenesis of inflammatory bowel disease(28, 29). However, whether SERPINE1 regulates cellular senescence through the cGAS-STING pathway remains unknown.

Here, by performing single-cell transcriptomic profiling of intestinal tissues from CD patients, we identified a previously uncharacterized subpopulation of SERPINE1$^+$ fibroblasts that exhibit a high senescence score, G1 cell-cycle arrest, and a pro-inflammatory secretory phenotype. These cells are almost exclusively localized to inflamed regions and function as central communication hubs, particularly interacting with IL1RN$^+$ macrophages. Through integrative ligand-receptor analysis and functional experiments, we demonstrate that IL1RN$^+$ macrophages drive fibroblast senescence via paracrine TNF-α signaling, and that SERPINE1 sustains this senescent phenotype by activating the cGAS-STING pathway. Importantly, pharmacological inhibition of SERPINE1 with TM5441 alleviates experimental colitis and suppresses cGAS-STING-mediated senescence in vivo. Collectively, our findings demonstrate that SERPINE1 drives pathogenic fibroblast senescence in Crohn's disease by activating the cGAS-STING pathway, thereby highlighting SERPINE1 as a key mediator of senescence and a potential therapeutic target in CD.

Methods

Data collection and processing

In this study, single-cell and bulk transcriptomic data for this study were obtained from the Gene Expression Omnibus (GEO) (https://www.ncbi.nlm.nih.gov/geo/). The scRNA-seq dataset (GSE134809) includes paired resection ileal samples from 11 patients, which included both inflamed and uninflamed tissues. Bulk RNA-seq data were sourced from four independent cohorts (GSE102133, GSE100833, GSE66407, GSE186582, andGSE16879) for biomarker validation.

For scRNA-seq processing, low-quality cells and doublets were filtered out using the following criteria: mitochondrial gene percentage < 20%, number of detected genes (nFeature_RNA) between 300 and 6,000, and removal of doublets with DoubletFinder (v2.0.6). After these filters, a total of 87,011 high-quality cells were retained for subsequent analysis. We then processed the data using the Seurat pipeline(30). Gene expression was log-normalized and scaled, and the top 3000 highly variable genes were selected for downstream analysis. Principal component analysis (PCA) was used for initial dimensionality reduction, and batch effects were corrected using Harmony (v1.2.3)(31). Uniform manifold approximation and projection (UMAP) was used for dimensionality reduction. Cell clustering was conducted using the FindClusters function (resolution = 0.3). Cell types were manually annotated based on the expression of canonical marker genes.

Quantification of senescence signature

In this study, we employed a senescence-associated gene set (SenMayo), described by Saul et al(32). This gene set has been confirmed to be enriched in senescent cells across various tissues and organisms. Enrichment analysis for the SenMayo gene set was performed on the scRNA-seq data using AUCell (v1.28.0). The complete gene list is provided in Supplemental Table S1.

Deconvolution of bulk transcriptomes

To infer the abundances of fibroblast subpopulations (including the SERPINE1 + subset) in independent bulk RNA-seq cohorts, we performed deconvolution analysis using CIBERSORTx (https://cibersortx.stanford.edu/)(33, 34). A custom signature matrix was generated from our scRNA-seq data. This signature and the bulk expression matrices (datasets GSE102133, GSE100833, and GSE186582) were then analyzed using the CIBERSORTx web portal with batch correction enabled and 100 permutations.

Cell–cell communication analysis using CellChat

To explore cell-cell interactions between different cell types, we used the CellChat package (v2.2.0)(35), which is based on known interactions between signaling ligands, receptors, and their cofactors

developed by Jin. et al. Secreted Signaling, ECM-Receptor, and Cell-Cell Contact relationships were considered. All analyses were performed using default parameters.

Nichenet

To infer signaling interactions between specific cell types and identify ligands that regulate gene expression changes in receiver cells, we applied NicheNet (v2.2.1)(36, 37) for cell-cell communication analysis. This method integrates prior knowledge of ligand–receptor interactions and intracellular signaling to predict ligands influencing target gene expression in receiver cells, along with their downstream signaling mediators.

In our study, we defined fibroblasts as the receiver cell population and macrophages as sender cells. The gene sets of interest consisted of genes differentially expressed in fibroblasts from inflammatory regions compared to those from uninflamed tissues.

Mice

All animal experiments were approved by the Experimental Animal Welfare Ethics Committee, Zhongnan Hospital of Wuhan University (WP20260092) and conducted in accordance with the Chinese regulations for the administration of laboratory animals. Male C57BL/6J mice (7 weeks, 20–22 g) were obtained from Sibefu (Beijing, China) and housed under standard specific pathogen-free (SPF) conditions. Mice were randomly assigned to three groups: wild-type (WT) control, DSS-induced colitis model, and TM5441 treatment. Colitis was induced by 2.5% DSS in drinking water for 7 days. During this period, the TM5441 group received daily intraperitoneal injections of TM5441(15mg/kg), followed by normal drinking water. All mice were euthanized on day 10.

During the experiment, the disease activity index (DAI) was calculated daily based on body weight loss, fecal bleeding, and stool consistency. On day 10, colon lengths were measured. Distal colon tissues were fixed in 4% paraformaldehyde and embedded in paraffin. Tissue sections were prepared and subjected to H&E staining by Beijing Saveir Biotechnology Co., Ltd. (Beijing, China).

Cell culture and co-culture experiments

RAW264.7 macrophages and CCD-18Co fibroblasts were maintained in complete DMEM (10% FBS, 1% P/S) at 37°C with 5% CO_2 and routinely tested for mycoplasma. To establish the co-culture system, RAW264.7 cells were polarized to an M1 phenotype using LPS (100 ng/mL, 24 h, Sigma-Aldrich, L4391). The conditioned medium (CM) from these M1 macrophages was collected, centrifuged, and applied to CCD-18Co fibroblasts for 48 h. For direct ligand stimulation, fibroblasts were treated with recombinant TNF-α (10 ~ 40 ng/mL, 24 h). Control groups included untreated fibroblasts and those exposed to CM from unstimulated (M0) macrophages.

Quantitative real-time PCR (qRT—PCR)

Total RNA was isolated with TRIzol (Invitrogen) and quantified. One microgram of RNA was reverse-transcribed into cDNA using the PrimeScript RT reagent Kit (Takara). qPCR was carried out in 20-μL reactions containing SYBR Green Supermix (Bio-Rad) on a CFX96 Real-Time PCR System (Bio-Rad). All reactions were performed in triplicate. Relative mRNA expression was analyzed using the 2 − ΔΔCt method, with GAPDH as the endogenous control. Primer sequences are detailed in the Supplementary Material.

Western Blot

The cells were lysed in RIPA buffer (NCM Biotech, China) containing protease inhibitors (NCM Biotech, China). Protein concentrations were quantified using a BCA protein assay kit (Beyotime, China). The primary antibodies used in this study included SERPINE1 (1:2000, genuin biotech Cat# 63098), CDKN1A (1:2000, genuin biotech Cat# 61661), CDKN2A (1:2000, genuin biotech Cat# 71177), and GAPDH (1:3000, Proteintech Cat# 60004-1-Ig).

Statistical analysis

Data are presented as the mean ± standard error of the mean (SEM) from at least three independent experiments. Statistical comparisons between two groups were performed using an unpaired two-tailed Student's t-test for data meeting assumptions of normality and equal variance, or the non-parametric Mann-Whitney U test (Wilcoxon rank-sum test) otherwise. A p-value of less than 0.05 was considered statistically significant. Significance levels are denoted as follows: * for $p < 0.05$, ** for $p < 0.01$, *** for $p < 0.001$, and **** for $p < 0.0001$.

Results

Landscape of Senescence genes in the scRNA-seq dataset for Crohn's Disease

To explore the landscape of cellular senescence genes (CSG) in crohn's disease (CD), we conducted deep analysis in single-cell sequencing data. After quality control, a total of 87011 cells were included for further scRNA-seq analysis. After dimensionality reduction and clustering, we annotated the cell clusters with detailed marker information, identifying 10 major cell lineages (Fig. 1A). Batch effect correction was performed across all samples using harmony (v1.2.3) (Fig. 1B), showing that the overall distribution was relatively stable, and sensitivity to batch effects was minimal. Then, we calculated the percentage of these cell types in the two groups, the proportion of them varied across samples (Fig. 1C). Bubble plots displayed the expression proportion of significant marker genes across distinct cell types (Fig. 1D). To quantify senescence heterogeneity across cell populations, we performed AUCell scoring on each cell type using 125 CSG obtained from the Senmayo database, a reliable resource for curated cell senescence gene sets. Notably, fibroblasts and myeloid cells exhibited higher senescence scores and

demonstrated the most significant differences ($p < 0.0001$) between inflammatory and normal groups (Fig. 1E, F). However, due to the inherent challenge in distinguishing the senescence state of myeloid cells—as their secretion of proinflammatory factors overlap extensively with the senescence-associated secretory phenotype (SASP) and the highest average senescence score observed in fibroblasts, we prioritized the fibroblast population for further analysis, considering their potential involvement in CD pathogenesis.

Figure 1. Landscape of Senescence genes in the scRNA-seq dataset for Crohn's Disease. (A) UMAP visualization of major cell lineages. (B) UMAP visualization after batch-effect correction. (C) Stacked bar plot displaying proportional composition of major cell types between involved and uninvolved tissue. (D) Dot plot of canonical marker-gene expression used for cell-type annotation (size = percent expressed; color = mean level). (E-F) Violin and UMAP plots of senescence (Senmayo gene-set) AUCell scores, showing cell-type and group differences (E) and global distribution (F).

SERPINE1⁺ fibroblasts represent inflammation- specific senescent cells driving disease pathogenesis

Based on elevated senescence scores in inflammatory versus normal fibroblasts, we subclustered fibroblasts into 5 transcriptionally distinct subpopulations (Fig. 2A), consistent with recent studies identifying multiple subsets in CD strictures and mucosa(38). Marker gene expression is shown in Fig. 2B. AUCell-based senescence scoring revealed SERPINE1⁺ fibroblasts exhibited the highest scores (Fig. 2D). Consistent with cellular senescence—characterized by G1 arrest, apoptosis resistance, and SASP(39, 40) —scran analysis showed SERPINE1⁺ fibroblasts were almost entirely arrested in G1, unlike actively cycling other subclusters(41, 42) (Fig. 2D). These cells were primarily enriched in inflammatory regions and nearly absent in normal tissues (Fig. 2E), aligning with reported roles of SERPINE1/PAI-1 in intestinal fibrosis (43).

CIBERSORTx deconvolution of public datasets (GSE102133, GSE100833, GSE186582)(34) validated these findings: SERPINE1⁺ fibroblasts were almost exclusively detected in CD samples versus controls (Figs. 2F–2H). Given SERPINE1/PAI-1 is an established senescence-associated gene(44), these data identify SERPINE1⁺ fibroblasts as a senescent, cell cycle-arrested subpopulation contributing to chronic CD inflammation.

Pathway enrichment (GO, KEGG, Hallmark) revealed ECM organization and apoptotic regulation (GO), neurodegenerative disease pathways (KEGG)—possibly reflecting shared oxidative stress mechanisms—and robust Hallmark enrichments in inflammatory response, TNF-α signaling via NF-κB(45), and hypoxia (46) (Fig. 2I). The co-enrichment of hypoxia and inflammation mirrors the CD microenvironment and drives senescence/SASP.

Collectively, this functional signature—marked by inflammatory activation and hypoxic response—underpins the senescent state of SERPINE1⁺ fibroblasts. Their robust SASP profile and near-exclusive

localization to inflamed tissues suggest these cells function as "inflammatory amplifiers" perpetuating chronic mucosal inflammation and tissue pathogenesis in CD.

Figure 2. SERPINE1⁺ fibroblasts represent inflammation- specific senescent cells driving disease pathogenesis. (A) UMAP plots of the subclustered fibroblasts. (B) Heatmap of discriminative marker genes used to define fibroblast subclusters. (C) Violin plot of Senmayo (senescence) AUCell scores across fibroblast subpopulations. (D) Stacked bar chart of cell-cycle phase distributions across fibroblast subclusters. (E) Stacked bar plot showing proportional abundance of fibroblast subclusters between involved and uninvolved groups. (F-H) Box plots of CIBERSORTx-deconvolved SERPINE1 + fibroblast proportions in three independent GEO datasets (GSE100833, GSE102133, GSE186582), comparing Crohn's disease (CD) versus control tissue. (I) GO, KEGG and GSEA enrichment results for the SERPINE1 + fibroblast gene set.

SERPINE1 + Fibroblasts Function as Communication Hubs in Crohn's Disease

To map intercellular communication networks in CD, we applied CellChat to all cellular populations. Fibroblasts engaged in the majority of communications (Fig. 3A). Comparing inflamed versus normal tissues, CEACAM, COMPLEMENT, MIF, ICAM, and COLLAGEN pathways were enriched in inflammation, whereas GDNF, EGF, NOTCH, and VEGF predominated in normal regions (Supplementary Fig. 1A). Notably, COLLAGEN, CypA, and MIF pathways were exclusive to the inflammatory group (Fig. 3B).

Within the MIF pathway—where pro-inflammatory cytokine MIF triggers NF-κB, AKT, and AMPK signaling(47)—SERPINE1⁺ fibroblasts served as primary senders, with B cells and myeloid cells as main receivers (Supplementary Fig. 1B), suggesting these fibroblasts drive inflammatory microenvironments through immune cell interactions.

Comparative analysis revealed SERPINE1⁺ fibroblasts exhibited significantly more interactions than SERPINE1⁻ fibroblasts, preferentially connecting to myeloid cells, B cells, endothelial cells, and stem cells (Fig. 3C). SERPINE1⁺ fibroblasts displayed the highest outgoing communication strength and substantial incoming activity, while myeloid cells showed the highest incoming intensity (Fig. 3D). These findings suggest SERPINE1⁺ fibroblasts remodel the immune microenvironment via enhanced communication, particularly through SASP factors targeting myeloid and lymphoid lineages.

Given the strong fibroblast-myeloid communication, we subclustered myeloid populations for refined analysis (Fig. 3E; transcriptional signatures in Supplementary Fig. 1C). CellChat revealed extensive, heterogeneous networks between fibroblast subtypes and myeloid cells (Fig. 3F). SERPINE1⁺ fibroblasts emerged as the most interactive subset, with both highest outgoing strength and greater incoming activity than SERPINE1⁻ fibroblasts (Fig. 3G). They exhibited significantly stronger communication with all myeloid subpopulations (Fig. 3H), with the most robust interaction specifically occurring between SERPINE1⁺ fibroblasts and IL1RN⁺ macrophages—implicating this axis as critical to the CD microenvironment.

Figure 3. SERPINE1 + Fibroblasts Function as Communication Hubs in Crohn's Disease. (A) CellChat circle plot of global intercellular communication networks. (B) Differential cell-cell communication strength between involved and uninvolved fibroblasts. (C) Circle plot comparing inter-cell-type communication strengths between SERPINE1 + and SERPINE1 − fibroblasts. (D) Dotplot of total outgoing and incoming signaling strength for each cell population, highlighting SERPINE1 + fibroblasts among the top communicators. (E) UMAP visualization of myeloid cell sub-clusters after re-clustering and annotation. (F) Circle plot summarizing global cell–cell communication between myeloid subsets and fibroblast subpopulations. (G) Dot plot comparing outgoing and incoming signaling strength among myeloid and fibroblast subpopulations. (H) Circle plot comparing communication strength between SERPINE1 + versus SERPINE1 − fibroblasts and individual myeloid subpopulations.

IL1RN+ Macrophages Drive Fibroblasts Senescence via TNF-α Signaling

Building on CellChat results, we employed NicheNet to predict ligand-receptor-target interactions between macrophages and SERPINE1⁺ fibroblasts, using differentially expressed fibroblast genes as the target set. The top 30 predicted macrophage ligands included IL1B, TGFB1, IL1A, CXCL12, IL6, and TNF (Fig. 5A; corresponding receptors in Supplementary Fig. 2A). Enrichment analysis of their predicted targets revealed significant involvement in apoptosis regulation, immune response, leukocyte chemotaxis, and TNF signaling (Supplementary Fig. 2B, C), underscoring their immunomodulatory roles.

To identify senescence-inducing ligands, we focused on senescence-associated genes (SAGs) within predicted targets and traced their upstream regulators. IL1B, IL1A, TGFB1, and TNF emerged as master regulators of fibroblast senescence (Fig. 5C). Notably, these ligands were specifically enriched in IL1RN⁺ macrophages (Fig. 5D), with their activity strongly correlating with fibroblast senescence scores ($r = 0.8$, $p = 0.001$; Fig. 5E). This independently corroborates CellChat findings, identifying IL1RN⁺ macrophages as key drivers of fibroblast senescence via paracrine signaling (Fig. 5F).

Given that IL1B, TGFB1, and TNF upregulate SERPINE1 in fibroblasts (Fig. 5B-C), and TNF expression in IL1RN⁺ macrophages showed the strongest correlation with fibroblast senescence ($r = 0.56$, $p = 0.031$; Fig. 5G), we hypothesize TNF-α as the primary pro-senescence signal from IL1RN⁺ macrophages to SERPINE1⁺ fibroblasts. This aligns with TNF-α's established role in senescence and SASP induction, with CellChat confirming IL1RN⁺ macrophages as predominant TNF signal senders and SERPINE1⁺ fibroblasts as major receivers.

Collectively, our integrated analyses support a model wherein IL1RN⁺ macrophages drive senescent and pro-fibrotic phenotypes in SERPINE1⁺ fibroblasts through paracrine TNF-α (and potentially IL1B), thereby contributing to Crohn's disease pathogenesis.

Figure 4. IL1RN+ Macrophages Drive Fibroblasts Senescence via TNF-α Signaling. (A-B) Heatmap showing the activity of ligands inferred to regulate SERPINE1 + fibroblasts by myeloid subsets (A), the predicted downstream target genes within SERPINE1 + fibroblasts (B). (C) Heatmap of ligand activities

and their predicted senescence-associated target genes in fibroblasts, ranked by regulatory potential. (D) Dot plot showing expression (size = percent expressed; color = mean level) of key ligands across myeloid sub-populations. (E) Scatterplot showing the positive correlation between IL1RN+ macrophage ligand activity and fibroblast senescence score across samples (r = 0.80, p = 0.001). (F) Heatmap of the TNF signaling pathway highlighting the main sender and receiver cell populations inferred by CellChat. (G) Scatterplots showing correlations between IL1RN+ macrophage expression of TNF, IL1B and TGFB1 (x-axis) and fibroblast senescence score (y-axis); TNF exhibits a significant positive correlation (r = 0.56, p = 0.031), whereas IL1B and TGFB1 show no significant association.

SERPINE1 drives cGAS-STING-mediated cellular senescence and pro-inflammatory signaling in Crohn's disease

To evaluate SERPINE1 as a biomarker in Crohn's disease (CD), we analyzed multiple independent RNA-seq cohorts and observed robust upregulation of SERPINE1 in diseased tissues (Fig. 5A; GSE102133, GSE66407, GSE186582). SERPINE1 demonstrated high diagnostic accuracy across all three datasets (AUC > 0.8), supporting its potential as a diagnostic biomarker (Fig. 6B). This transcriptional increase was corroborated by elevated protein levels in Western blot analysis (Fig. 5C-D).

To assess the clinical relevance of SERPINE1$^+$ fibroblasts, we performed CIBERSORTx deconvolution on a bulk RNA-seq dataset from Infliximab-treated CD patients (GSE16879). Baseline proportions of SERPINE1$^+$ fibroblasts were significantly higher in non-responders than in responders (Supplementary Fig. 3A; p = 0.00078), suggesting this subpopulation predicts therapeutic resistance. To investigate functional roles, we generated SERPINE1 knockdown CCD-18Co fibroblasts (Supplementary Fig. 3B). Using a macrophage–fibroblast co-culture system, we found that M1-polarized RAW264.7 macrophages induced fibroblast senescence, marked by upregulation of CDKN1A, CDKN2A, and SERPINE1 (Fig. 5F). TNF-α, identified by NicheNet as a top ligand, independently upregulated SERPINE1, validating the predicted signaling axis (Supplementary Fig. 3C). These senescent fibroblasts concurrently expressed pro-inflammatory SASP factors (Supplementary Fig. 3E), indicating that SERPINE1-driven senescence may contribute to disease progression primarily by promoting local inflammatory signaling within the CD microenvironment.

Previous studies have recognized SERPINE1 as both a marker and mediator of senescence (17, 48, 49). To elucidate its underlying regulatory mechanism in our system, we performed knockdown experiments in M1-treated cells. SERPINE1 depletion partially rescued M1-induced senescence, as evidenced by the downregulated expression of CDKN1A and CDKN2A (Fig. 5E-F), alongside a concomitant reduction in key SASP factors, including IL6, IL8, and CCL2 (Supplementary Fig. 3E). These findings reinforce the role of SERPINE1 as a critical regulator that sustains senescence and its pro-inflammatory output within the CD microenvironment.

Recently, the cGAS-STING signaling axis has emerged as a pivotal node bridging innate immune sensing to cellular senescence(50, 51). Driven by the aberrant accumulation of cytosolic DNA, this pathway incites potent inflammatory cascades and reinforces senescent phenotypes. We thus investigated whether SERPINE1 engages this pathway in CD. Transcriptomic analysis revealed a strong positive correlation between SERPINE1 and STING (TMEM173) expression (Fig. 5G; $r = 0.67$, $p < 0.001$), indicating a potential regulatory link between SERPINE1 and cGAS-STING signaling. SERPINE1 knockdown in CCD-18Co cells led to a marked reduction in the phosphorylation levels of STING, TBK1, and IRF3 (Fig. 5H, I). Consistently, pharmacological inhibition of SERPINE1 with TM5441 yielded similar results (Fig. 5H, I). SERPINE1 overexpression exerted the opposite effect, promoting the phosphorylation of these key components (Fig. 5J-K). Inhibiting STING with C170 suppressed this pathway activation and partially rescued SERPINE1-induced senescence (Fig. 5J, K). Together, these findings demonstrate that SERPINE1 drives cellular senescence and cytokine secretion, at least in part, by promoting cGAS-STING activation.

Figure 5. SERPINE1 drives cGAS-STING-mediated cellular senescence and pro-inflammatory signaling in Crohn's disease (A) SERPINE1 expression is significantly elevated in CD patients across three public datasets. (B) SERPINE1 shows strong diagnostic performance (AUC > 0.8) across three datasets. (C-D) Elevated SERPINE1 protein expression in human intestinal tissues from CD. (E-F) SERPINE1 knockdown suppresses M1 macrophage-fibroblast co-culture-induced inflammatory SASP expression. (G) correlation between SERPINE1 and TMEM173 (STING) expression in Crohn's disease (GSE75214). Pearson correlation coefficient $R = 0.67$, $p < 2.2 \times 10^{-16}$. (H-I) SERPINE1 knockdown and pharmacological inhibition attenuate cGAS-STING pathway activation. (J-K) SERPINE1 overexpression promotes cGAS-STING pathway activation, and STING inhibition rescues SERPINE1-induced senescence.

Validating Serpine1 as a DSS therapeutic target using TM5441

To validate our in vitro findings and evaluate SERPINE1 as a therapeutic target, we administered the SERPINE1 inhibitor TM5441 in a DSS-induced colitis model. Wild-type mice were randomized into three groups: control, DSS, and DSS + TM5441. Mice in the DSS and treatment groups received 2.5% DSS in drinking water for 7 days, with concurrent daily TM5441 administration beginning at the onset of DSS exposure (Fig. 6A). Throughout the experimental period, mice were monitored for clinical parameters including body weight and disease activity. Compared with DSS-treated controls, TM5441-treated mice exhibited reduced colon shortening (Fig. 6B, D), markedly attenuated weight loss (Fig. 6E), and significantly lower disease activity index (DAI) scores (Fig. 6F). Histological examination by H&E staining further revealed that TM5441 treatment substantially ameliorated mucosal architecture disruption and diminished inflammatory cell infiltration (Fig. 6C). These findings demonstrate that pharmacological inhibition of SERPINE1 confers protective effects against DSS-induced colonic injury, supporting SERPINE1 as a viable therapeutic target in inflammatory bowel disease.

To elucidate the molecular mechanism underlying these protective effects, we examined cGAS-STING pathway activity in colonic tissues. Western blotting showed that TM5441 inhibited SERPINE1 expression, confirming its on-target inhibitory effect. In vivo, TM5441-mediated cGAS-STING inactivation suppressed downstream STING, TBK1, and IRF3 phosphorylation. This validates that pharmacological SERPINE1 inhibition blocks cGAS-STING activation in vivo, thereby alleviating DSS-induced colitis.

Figure 6. Validating Serpine1 as a DSS therapeutic target using TM5441 (A) Schematic overview of the experimental design using the selective SERPINE1 inhibitor TM5441 in the DSS-induced mouse model. (B) Representative photographs of colons. (C) H&E staining of colon sections. Scale bar: 200 μm (or 50 μm for enlarged regions). (D) Quantification of colon length. (E) Body weight trajectories demonstrate that TM5441 treatment significantly attenuates DSS-induced weight loss. (F) Disease activity index (DAI) score. (G) TM5441 significantly inhibits STING pathway activation in DSS-treated mice.

Discussion

CD is marked by dysfunctional and overactive immune responses that lead to uncontrolled inflammation(52). Emerging evidence indicates that cellular senescence and the SASP perpetuate chronic inflammation across a spectrum of inflammatory diseases(53, 54). Senescent cells maintain and regulate the SASP through pathways such as NF-κB, JAK2/3, p38 MAPK, and cGAS-STING, thereby sustaining the inflammatory tissue microenvironment(53). However, the specific molecular drivers of fibroblast senescence in CD remain poorly defined. In this study, we demonstrate that SERPINE1 is upregulated in CD and drives cellular senescence and inflammation. Single-cell transcriptomic analysis identified fibroblasts as the cell population exhibiting the most pronounced senescence signature and revealed SERPINE1 as a key senescence-associated marker in this population. In vitro, SERPINE1 knockdown in fibroblasts attenuated cellular senescence and reduced the secretion of SASP-related inflammatory factors.

Senescence and the pro-inflammatory SASP drive chronic inflammation and disease (10, 55, 56). Although therapeutic targeting of senescence and SASP has shown promise in other diseases (9, 57), its contribution to CD pathogenesis remains incompletely understood. Increasing evidence supports the involvement of the cGAS-STING pathway in IBD pathogenesis(29, 58). In CD, STING expression was elevated in the colon and the cGAS-STING pathway was highly activated(59, 60). Moreover, dsDNA-loaded EVs activate macrophage STING signaling, driving CD progression(59). Necroptotic MLKL activation damages mitochondria, releasing mtDNA into the cytosol to engage the cGAS-STING pathway and amplify intestinal inflammation(61). Thus, cGAS-STING-mediated inflammation and cellular senescence may contribute to the chronic progression of CD.

In our study, single-cell analysis revealed an enrichment of SERPINE1^{+} fibroblasts in CD, which was corroborated by marked upregulation of SERPINE1 protein as determined by Western blotting. Although PAI-1 induces cellular senescence in multiple contexts(18, 20, 62), the molecular mechanisms governing this process remain elusive. PAI-1 knockdown or TM5441 treatment in CCD-18Co cells suppressed

STING phosphorylation and downstream signaling, whereas PAI-1 overexpression potentiated STING activation, implicating PAI-1 as a positive regulator of the cGAS-STING pathway. Consistent with previous studies(17, 20, 62), PAI-1 overexpression upregulated p21 expression, a canonical senescence marker(63), indicative of enhanced senescence induction. Notably, this effect was partially abrogated by C-176, a pharmacological inhibitor of the STING pathway, suggesting that PAI-1 promotes cellular senescence, at least in part, through the cGAS-STING axis. Further mechanistic studies are warranted to elucidate how PAI-1 engages and activates the STING pathway.

The DSS-induced colitis model is one of the most widely used models in gastrointestinal inflammation research. In our model, DSS administration induced severe colonic inflammation characterized by marked weight loss, persistent diarrhea, and rectal bleeding. Treatment with TM5441, a pharmacological inhibitor of PAI-1, significantly attenuated disease severity. This protective effect was associated with preserved epithelial barrier integrity and reduced inflammatory cell infiltration in the mucosa and submucosa. Given the established role of cGAS-STING signaling in driving IBD pathogenesis(29), we examined whether TM5441 modulates this axis. Mechanistically, TM5441 diminished phosphorylation of STING, TBK1, and IRF3, indicating suppression of cGAS-STING pathway activation. Collectively, TM5441 protects against colitis, at least in part, by blocking cGAS-STING-mediated inflammation and senescence.

This study has several limitations. First, the DSS-induced colitis model, although widely used, is an acute chemical injury model and does not fully recapitulate the chronic relapsing-remitting nature of human Crohn's disease. Second, TM5441 is a pharmacological inhibitor of SERPINE1/PAI-1; potential off-target effects cannot be completely excluded. Third, we demonstrated that TM5441 suppressed the phosphorylation of STING, TBK1, and IRF3, suggesting cGAS-STING pathway inhibition; however, more direct evidence, such as genetic deletion of STING or SERPINE1, is needed to establish a definitive causal link. Finally, the precise molecular mechanism by which SERPINE1 activates the cGAS-STING pathway remains to be elucidated. These limitations should be addressed in future studies.

Collectively, our study identifies SERPINE1 as a central regulator of fibroblast senescence and inflammation in the CD mucosal microenvironment, with the cGAS-STING axis serving as a critical downstream mediator of SERPINE1-driven SASP. These findings provide novel mechanistic insights into CD pathogenesis and suggest that pharmacological inhibition of SERPINE1 may offer a viable therapeutic approach for managing intestinal inflammation in CD.

Abbreviations

CD
Crohn’s disease
IBD
Inflammatory bowel disease
HC

Healthy control

SASP

Senescence-associated secretory phenotype

PAI-1

Plasminogen activator inhibitor-1

SERPINE1

Serpin family E member 1

TNF-α

Tumor necrosis factor-alpha

scRNA-seq

Single-cell RNA sequencing

SenMayo

A specific gene set used to identify senescent cells

GSVA

Gene set variation analysis

KEGG

Kyoto Encyclopedia of Genes and Genomes

GO

Gene Ontology

DSS

Dextran sulfate sodium

EVs

Extracellular vesicles

mtDNA

Mitochondrial DNA

AUC

Area under the curve

Declarations

Conflict of interest statement

The authors have no relevant financial or non-financial interests to disclose.

Ethics approval and consent to participate

All human tissue research in this study obtained approval from the Medical Ethics Committee, Zhongnan Hospital of Wuhan University (2025003K) and performed in accordance with the Declaration of Helsinki.

All participants provided informed consent. Animal experiments procedures were approved by the Experimental Animal Welfare Ethics Committee, Zhongnan Hospital of Wuhan University (WP20260092).

Funding

This study was funded by the National Natural Science Foundation of China (No. 82470556), Wuhan University Zhongnan Hospital Medical Science and Technology Innovation Platform Construction Support Key Project Fund (NO. PTXM2022007), Wuhan University Zhongnan Hospital Translational Medicine and Interdisciplinary Research Joint Fund (ZNJC202316).

Author Contribution

All authors contributed to the study conception and design. Pule Liu conducted the primary experiments, performed the core data analysis, and drafted the manuscript. Ruidong Wang contributed to the experimental work and RNA-seq data analysis, and assisted in preparing the initial draft. Yali Yu contributed to statistical analysis and visualization. Yumei Ning participated in the literature search and interpreted the bioinformatic results. Mei Ye and Minhu Chen were responsible for funding acquisition and study supervision. Mei Ye, as the lead corresponding author, guided the selection of analytical strategies. All authors have read and approved the final manuscript.

Acknowledgment

Declared none.

Data availability statement

All public datasets enrolled in this study were downloaded from the Gene Expression Omnibus (GEO) database (https://www.ncbi.nlm.nih.gov/geo/). Specifically, the single-cell RNA sequencing data (GSE134809) and multiple bulk transcriptomic cohorts (GSE102133, GSE100833, GSE66407, GSE186582, and GSE16879) were utilized for analysis and validation. All data generated or analyzed during this study, including processed gene sets and supplemental tables, are included in the supplementary information files of this article.

References

1. Lee M, Chang EB. Inflammatory Bowel Diseases (IBD) and the Microbiome-Searching the Crime Scene for Clues. Gastroenterology. 2021;160(2):524–37. 10.1053/j.gastro. .2020.09.056 PubMed PMID: 33253681; PubMed Central PMCID: PMC8098834.

2. Caruso R, Lo BC, Núñez G. Host-microbiota interactions in inflammatory bowel disease. Nat Rev Immunol. 2020;20(7):411–26. 10.1038/s41577-019-0268-7 . PubMed PMID: 32005980.
3. Martin JC, Chang C, Boschetti G, Ungaro R, Giri M, Grout JA, et al. Single-Cell Analysis of Crohn's Disease Lesions Identifies a Pathogenic Cellular Module Associated with Resistance to Anti-TNF Therapy. Cell. 2019;178(6):1493–e150820. 10.1016/j.cell.2019.08.008 . PubMed PMID: 31474370; PubMed Central PMCID: PMC7060942.
4. Feng J, He LN, Yao R, Qiao Y, Yang T, Cui Z, et al. Comprehensive analysis of heterogeneity and cell-cell interactions in Crohn's disease reveals novel location-specific insights. J Adv Res. 2025;76:679–94. 12.042 PubMed PMID: 39732334.
5. Mitsialis V, Wall S, Liu P, Ordovas-Montanes J, Parmet T, Vukovic M, et al. Single-Cell Analyses of Colon and Blood Reveal Distinct Immune Cell Signatures of Ulcerative Colitis and Crohn's Disease. Gastroenterology. 2020;159(2):591–e60810. 10.1053/j.gastro.2020.04.074 . PubMed PMID: 32428507; PubMed Central PMCID: PMC8166295.
6. Yanai H, Hanauer SB. Assessing response and loss of response to biological therapies in IBD. Am J Gastroenterol. 2011;106(4):685–98. 10.1038/ajg.2011.103 . PubMed PMID: 21427713.
7. Kennedy NA, Heap GA, Green HD, Hamilton B, Bewshea C, Walker GJ, et al. Predictors of anti-TNF treatment failure in anti-TNF-naive patients with active luminal Crohn's disease: a prospective, multicentre, cohort study. Lancet Gastroenterol Hepatol. 2019;4(5):341–53. 10.1016/S2468-1253.(19)30012-3 PubMed PMID: 30824404.
8. Calcinotto A, Kohli J, Zagato E, Pellegrini L, Demaria M, Alimonti A. Cellular Senescence: Aging, Cancer, and Injury. Physiol Rev. 2019;99(2):1047–78. 10.1152/physrev.00020.2018.
9. Baker DJ, Wijshake T, Tchkonia T, LeBrasseur NK, Childs BG, van de Sluis B, et al. Clearance of p16Ink4a-positive senescent cells delays ageing-associated disorders. Nature. 2011;479(7372):232–6. 10.1038/nature10600 . PubMed PMID: 22048312; PubMed Central PMCID: PMC3468323.
10. Wang B, Han J, Elisseeff JH, Demaria M. The senescence-associated secretory phenotype and its physiological and pathological implications. Nat Rev Mol Cell Biol. 2024;25(12):958–78. 10.1038/s41580-024-00727-x.
11. Popp C, Nichita L, Voiosu T, Bastian A, Cioplea M, Micu G, et al. Expression Profile of p53 and p21 in Large Bowel Mucosa as Biomarkers of Inflammatory-Related Carcinogenesis in Ulcerative Colitis. Dis Markers. 2016;2016:3625279. 10.1155/2016/3625279 . PubMed PMID: 27578918; PubMed Central PMCID: PMC4992508.
12. Campisi J. Aging, cellular senescence, and cancer. Annu Rev Physiol. 2013;75:685–705. 10.1146/annurev-physiol-030212. -183653 PubMed PMID: 23140366; PubMed Central PMCID: PMC4166529.
13. Acosta JC, Banito A, Wuestefeld T, Georgilis A, Janich P, Morton JP, et al. A complex secretory program orchestrated by the inflammasome controls paracrine senescence. Nat Cell Biol.

2013;15(8):978–90. 10.1038/ncb2784 . PubMed PMID: 23770676; PubMed Central PMCID: PMC3732483.

14. Gorgoulis V, Adams PD, Alimonti A, Bennett DC, Bischof O, Bishop C, et al. Cellular Senescence: Defining a Path Forward. Cell. 2019;179(4):813–27. 10.1016/j.cell.2019.10.005 . PubMed PMID: 31675495.
15. Franceschi C, Garagnani P, Parini P, Giuliani C, Santoro A. Inflammaging: a new immune–metabolic viewpoint for age-related diseases. Nat Rev Endocrinol. 2018;14(10):576–90. 10.1038/s41574-018-0059-4.
16. Catarinella G, Nicoletti C, Bracaglia A, Procopio P, Salvatori I, Taggi M, et al. SerpinE1 drives a cell-autonomous pathogenic signaling in Hutchinson-Gilford progeria syndrome. Cell Death Dis. 2022;13(8):737. 10.1038/s41419-022-05168-y . PubMed PMID: 36028501; PubMed Central PMCID: PMC9418244.
17. Kortlever RM, Higgins PJ, Bernards R. Plasminogen activator inhibitor-1 is a critical downstream target of p53 in the induction of replicative senescence. Nat Cell Biol. 2006;8(8):877–84. 10.1038/ncb1448 . PubMed PMID: 16862142; PubMed Central PMCID: PMC2954492.
18. Muñoz-Espín D, Serrano M. Cellular senescence: from physiology to pathology. Nat Rev Mol Cell Biol. 2014;15(7):482–96. 10.1038/nrm3823 . PubMed PMID: 24954210.
19. Wan YZ, Gao P, Zhou S, Zhang ZQ, Hao DL, Lian LS, et al. SIRT1-mediated epigenetic downregulation of plasminogen activator inhibitor-1 prevents vascular endothelial replicative senescence. Aging Cell. 2014;13(5):890–9. 10.1111/acel.12247 . PubMed PMID: 25040736; PubMed Central PMCID: PMC4331759.
20. Jiang C, Liu G, Luckhardt T, Antony V, Zhou Y, Carter AB, et al. Serpine 1 induces alveolar type II cell senescence through activating p53-p21-Rb pathway in fibrotic lung disease. Aging Cell. 2017;16(5):1114–24. 10.1111/acel.12643 . PubMed PMID: 28722352; PubMed Central PMCID: PMC5595683.
21. Kortlever RM, Higgins PJ, Bernards R. Plasminogen activator inhibitor-1 is a critical downstream target of p53 in the induction of replicative senescence. Nat Cell Biol. 2006;8(8):877–84. 10.1038/ncb1448 . PubMed PMID: 16862142; PubMed Central PMCID: PMC2954492.
22. Eren M, Boe AE, Murphy SB, Place AT, Nagpal V, Morales-Nebreda L, et al. PAI-1-regulated extracellular proteolysis governs senescence and survival in Klotho mice. Proc Natl Acad Sci U S A. 2014;111(19):7090–5. 10.1073/pnas.1321942111 . PubMed PMID: 24778222; PubMed Central PMCID: PMC4024885.
23. Botla SK, Savant S, Jandaghi P, Bauer AS, Mücke O, Moskalev EA, et al. Early Epigenetic Downregulation of microRNA-192 Expression Promotes Pancreatic Cancer Progression. Cancer Res. 2016;76(14):4149–59. 10.1158/0008-5472. .CAN-15-0390 PubMed PMID: 27216198.
24. Wang B, Gu B, Gao L, Ma C, Li X, Wang Y, et al. SERPINE1 Facilitates Metastasis in Gastric Cancer Through Anoikis Resistance and Tumor Microenvironment Remodeling. Small Weinh Bergstr Ger. 2025;21(19):e2500136. 10.1002/smll.202500136 . PubMed PMID: 40207795.

25. Yang H, Wang H, Ren J, Chen Q, Chen ZJ. cGAS is essential for cellular senescence. Proc Natl Acad Sci U S A. 2017;114(23):E4612–20. 10.1073/pnas.1705499114 . PubMed PMID: 28533362; PubMed Central PMCID: PMC5468617.
26. Takahashi A, Loo TM, Okada R, Kamachi F, Watanabe Y, Wakita M, et al. Downregulation of cytoplasmic DNases is implicated in cytoplasmic DNA accumulation and SASP in senescent cells. Nat Commun. 2018;9(1):1249. 10.1038/s41467-018-03555-8 . PubMed PMID: 29593264; PubMed Central PMCID: PMC5871854.
27. Glück S, Guey B, Gulen MF, Wolter K, Kang TW, Schmacke NA, et al. Innate immune sensing of cytosolic chromatin fragments through cGAS promotes senescence. Nat Cell Biol. 2017;19(9):1061–70. 10.1038/ncb3586 . PubMed PMID: 28759028; PubMed Central PMCID: PMC5826565.
28. Tao M, Wang L, Chen C, Tang M, Wang Y, Zhang J, et al. Developmentally endothelial locus-1 facilitates intestinal inflammation resolution by suppressing the Cmpk2-cGAS-STING pathway and promoting reparatory macrophage transition. J Adv Res. 2026;80:593–608. .030 PubMed PMID: 40288675; PubMed Central PMCID: PMC12869262.
29. Dimitrov G, Ryffel B, Togbe D, Quesniaux V. cGAS-STING DNA-sensing in inflammatory bowel diseases. Trends Mol Med. 2025;31(2):165–80. 10.1016/j.molmed.2024.10.002 . PubMed PMID: 39448330.
30. Butler A, Hoffman P, Smibert P, Papalexi E, Satija R. Integrating single-cell transcriptomic data across different conditions, technologies, and species. Nat Biotechnol. 2018;36(5):411–20. 10.1038/nbt.4096 . PubMed PMID: 29608179; PubMed Central PMCID: PMC6700744.
31. Korsunsky I, Millard N, Fan J, Slowikowski K, Zhang F, Wei K, et al. Fast, sensitive and accurate integration of single-cell data with Harmony. Nat Methods. 2019;16(12):1289–96. 10.1038/s41592-019-0619-0 . PubMed PMID: 31740819; PubMed Central PMCID: PMC6884693.
32. Saul D, Kosinsky RL, Atkinson EJ, Doolittle ML, Zhang X, LeBrasseur NK, et al. A new gene set identifies senescent cells and predicts senescence-associated pathways across tissues. Nat Commun. 2022;13(1):4827. 10.1038/s41467-022-32552-1 . PubMed PMID: 35974106; PubMed Central PMCID: PMC9381717.
33. Newman AM, Liu CL, Green MR, Gentles AJ, Feng W, Xu Y, et al. Robust enumeration of cell subsets from tissue expression profiles. Nat Methods. 2015;12(5):453–7. 10.1038/nmeth.3337 . PubMed PMID: 25822800; PubMed Central PMCID: PMC4739640.
34. Newman AM, Steen CB, Liu CL, Gentles AJ, Chaudhuri AA, Scherer F, et al. Determining cell type abundance and expression from bulk tissues with digital cytometry. Nat Biotechnol. 2019;37(7):773–82. 10.1038/s41587-019-0114-2 . PubMed PMID: 31061481; PubMed Central PMCID: PMC6610714.
35. Jin S, Guerrero-Juarez CF, Zhang L, Chang I, Ramos R, Kuan CH, et al. Inference and analysis of cell-cell communication using CellChat. Nat Commun. 2021;12(1):1088. 10.1038/s41467-021-21246-9 . PubMed PMID: 33597522; PubMed Central PMCID: PMC7889871.

36. Sang-Aram C, Browaeys R, Seurinck R, Saeys Y. Unraveling cell-cell communication with NicheNet by inferring active ligands from transcriptomics data. Nat Protoc. 2025;20(6):1439–67. 10.1038/s41596-024-01121-9 . PubMed PMID: 40038548.
37. Browaeys R, Saelens W, Saeys Y. NicheNet: modeling intercellular communication by linking ligands to target genes. Nat Methods. 2020;17(2):159–62. 10.1038/s41592-019-0667-5 . PubMed PMID: 31819264.
38. Mukherjee PK, Nguyen QT, Li J, Zhao S, Christensen SM, West GA, et al. Stricturing Crohn's Disease Single-Cell RNA Sequencing Reveals Fibroblast Heterogeneity and Intercellular Interactions. Gastroenterology. 2023;165(5):1180–96. 10.1053/j.gastro. .2023.07.014 PubMed PMID: 37507073.
39. Wang B, Han J, Elisseeff JH, Demaria M. The senescence-associated secretory phenotype and its physiological and pathological implications. Nat Rev Mol Cell Biol. 2024;25(12):958–78. 10.1038/s41580-024-00727-x.
40. Ajoolabady A, Pratico D, Bahijri S, Eldakhakhny B, Tuomilehto J, Wu F, et al. Hallmarks and mechanisms of cellular senescence in aging and disease. Cell Death Discov. 2025;11(1):364. 10.1038/s41420-025-02655-x . PubMed PMID: 40759632; PubMed Central PMCID: PMC12322153.
41. Lun ATL, McCarthy DJ, Marioni JC. A step-by-step workflow for low-level analysis of single-cell RNA-seq data with Bioconductor. F1000Research. 2016;5:2122. 10.12688/f1000research.9501.2 . PubMed PMID: 27909575; PubMed Central PMCID: PMC5112579.
42. Lun ATL, Bach K, Marioni JC. Pooling across cells to normalize single-cell RNA sequencing data with many zero counts. Genome Biol. 2016;17:75. 10.1186/s13059-016-0947-7 . PubMed PMID: 27122128; PubMed Central PMCID: PMC4848819.
43. De Santis S, Vidmar K, Williams J, Mattioli B, Chieppa M, Del Pinto R, UPREGULATION OF SERPINE1/PAI-1 INDUCED BY IL-33 CONTRIBUTES TO INTESTINAL FIBROSIS IN A CROHN'S DISEASE-LIKE ILEITIS MODEL. Gastroenterology. 2024;Abstracts From the 2024 Crohn's & Colitis Congress® Held January 25–27, 2024166(3, Supplement):S85. 10.1053/j.gastro.2023.11.193
44. Shaikh SB, Balaya RDA, Dagamajalu S, Bhandary YP, Unwalla H, Prasad TSK, et al. A signaling pathway map of plasminogen activator inhibitor-1 (PAI-1/SERPINE-1): a review of an innovative frontier in molecular aging and cellular senescence. Cell Commun Signal CCS. 2024;22(1):544. 10.1186/s12964-024-01910-5 . PubMed PMID: 39543686; PubMed Central PMCID: PMC11566301.
45. Fuhrmann-Stroissnigg H, Ling YY, Zhao J, McGowan SJ, Zhu Y, Brooks RW, et al. Identification of HSP90 inhibitors as a novel class of senolytics. Nat Commun. 2017;8(1):422. 10.1038/s41467-017-00314-z . PubMed PMID: 28871086; PubMed Central PMCID: PMC5583353.
46. Wiley CD, Campisi J. The metabolic roots of senescence: mechanisms and opportunities for intervention. Nat Metab. 2021;3(10):1290–301. 10.1038/s42255-. 021-00483-8 PubMed PMID: 34663974; PubMed Central PMCID: PMC8889622.
47. Kang I, Bucala R. The immunobiology of MIF: function, genetics and prospects for precision medicine. Nat Rev Rheumatol. 2019;15(7):427–37. 10.1038/s41584-019-0238-2.

48. Zhang D, Zhang JW, Xu H, Chen X, Gao Y, Jiang HG, et al. Therapy-induced senescent tumor cell-derived extracellular vesicles promote colorectal cancer progression through SERPINE1-mediated NF-κB p65 nuclear translocation. Mol Cancer. 2024;23:70. 10.1186/s12943-024-01985-1 . PubMed PMID: 38576002; PubMed Central PMCID: PMC10993572.
49. Ma YF, Qi ZR, Guo ZY, Yang JY, Ji MY, Chen SN, et al. Serpine1 as a potential therapeutic target in pyrrolidine alkaloids-induced hepatic sinusoidal obstruction syndrome. JHEP Rep. 2026;8(4):101736. 10.1016/j.jhepr.2026.101736 . PubMed PMID: 41783362; PubMed Central PMCID: PMC12955671.
50. Hy C, Wc H, Yc L, Hy L, Py L, Yt H, et al. Mitochondrial injury induced by a Salmonella genotoxin triggers the proinflammatory senescence-associated secretory phenotype. Nat Commun. 2024;15(1). 10.1038/s41467-024-47190-y . PubMed PMID: 38555361.
51. Y H, X L, S X, D Z, H L, H H, et al. Polyvinyl chloride nanoplastics suppress homology-directed repair and promote oxidative stress to induce esophageal epithelial cellular senescence and cGAS-STING-mediated inflammation. Free Radic Biol Med. 2025;226. 10.1016/j.freeradbiomed.2024.11.012 PubMed PMID: 39515594.
52. Khor B, Gardet A, Xavier RJ. Genetics and pathogenesis of inflammatory bowel disease. Nature. 2011;474(7351):307–17. doi:10.1038/nature10209 PubMed PMID: 21677747; PubMed Central PMCID: PMC3204665.
53. Han Z, Wang K, Ding S, Zhang M. Cross-talk of inflammation and cellular senescence: a new insight into the occurrence and progression of osteoarthritis. Bone Res. 2024;12:69. 10.1038/s41413-024-00375-z . PubMed PMID: 39627227; PubMed Central PMCID: PMC11615234.
54. Li X, Li C, Zhang W, Wang Y, Qian P, Huang H. Inflammation and aging: signaling pathways and intervention therapies. Signal Transduct Target Ther. 2023;8(1):239. 10.1038/s41392-023-01502-8 . PubMed PMID: 37291105; PubMed Central PMCID: PMC10248351.
55. Liu Z, Liang Q, Ren Y, Guo C, Ge X, Wang L, et al. Immunosenescence: molecular mechanisms and diseases. Signal Transduct Target Ther. 2023;8(1):200. 10.1038/s41392-023-01451-2 . PubMed PMID: 37179335; PubMed Central PMCID: PMC10182360.
56. López-Otín C, Blasco MA, Partridge L, Serrano M, Kroemer G. The hallmarks of aging. Cell. 2013;153(6):1194–217. 10.1016/j.cell. .2013.05.039 PubMed PMID: 23746838; PubMed Central PMCID: PMC3836174.
57. Childs BG, Gluscevic M, Baker DJ, Laberge RM, Marquess D, Dananberg J, et al. Senescent cells: an emerging target for diseases of ageing. Nat Rev Drug Discov. 2017;16(10):718–35. 10.1038/nrd.2017.116 . PubMed PMID: 28729727; PubMed Central PMCID: PMC5942225.
58. Tao M, Wang L, Chen C, Tang M, Wang Y, Zhang J, et al. Developmentally endothelial locus-1 facilitates intestinal inflammation resolution by suppressing the Cmpk2-cGAS-STING pathway and promoting reparatory macrophage transition. J Adv Res. 2026;80:593–608. .030 PubMed PMID: 40288675; PubMed Central PMCID: PMC12869262.

59. Extracellular vesicles package. dsDNA to aggravate Crohn's disease by activating the STING pathway | Cell Death & Disease [Internet]. [cited 2026 May 24]. Available from: https://www.nature.com/articles/s41419-021-04101-z
60. Frontiers. | Low-dose ganciclovir ameliorates dextran sulfate sodium-induced ulcerative colitis through inhibiting macrophage STING activation in mice [Internet]. [cited 2026 May 24]. Available from: https://www.frontiersin.org/journals/pharmacology/articles/10.3389/fphar.2022.1020670/full.
61. Ding Z, Wang R, Li Y, Wang X. MLKL activates the cGAS-STING pathway by releasing mitochondrial DNA upon necroptosis induction. Mol Cell. 2025;85(13):2610–e26255. 10.1016/j.molcel.2025.06.005 . PubMed PMID: 40614706.
62. Vaughan DE, Rai R, Khan SS, Eren M, Ghosh AK. Plasminogen Activator Inhibitor-1 Is a Marker and a Mediator of Senescence. Arterioscler Thromb Vasc Biol. 2017;37(8):1446–52. 10.1161/ATVBAHA.117.309451 . PubMed PMID: 28572158; PubMed Central PMCID: PMC5846199.
63. Wang B, Han J, Elisseeff JH, Demaria M. The senescence-associated secretory phenotype and its physiological and pathological implications. Nat Rev Mol Cell Biol. 2024;25(12):958–78. 10.1038/s41580-024-. 00727-x PubMed PMID: 38654098.

Figures

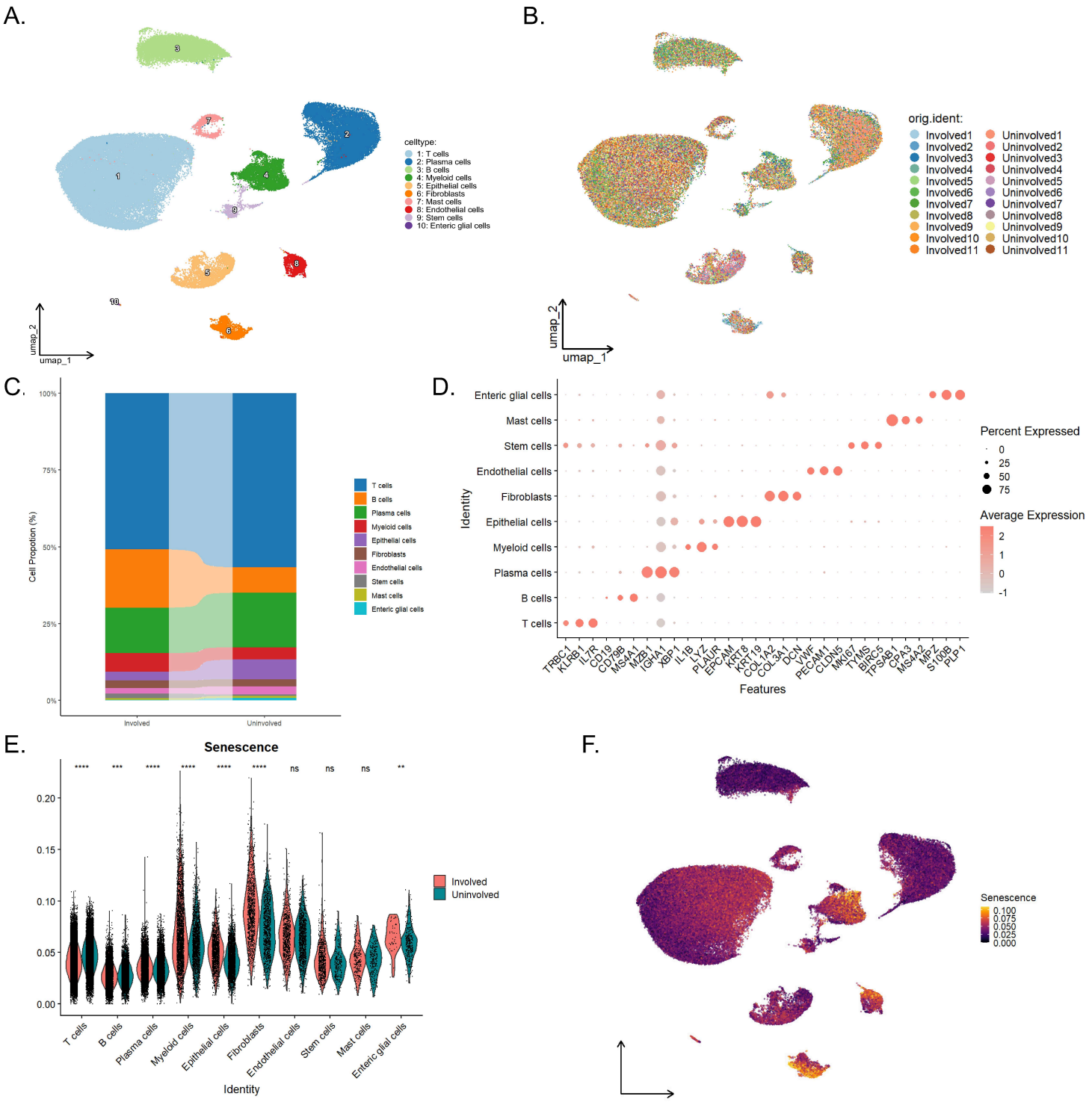


Figure 1

Landscape of Senescence genes in the scRNA-seq dataset for Crohn's Disease.(A) UMAP visualization of major cell lineages.(B) UMAP visualization after batch-effect correction. (C) Stacked bar plot displaying proportional composition of major cell types between involved and uninvolved tissue. (D) Dot plot of canonical marker-gene expression used for cell-type annotation (size = percent expressed; color =

mean level). (E-F) Violin and UMAP plots of senescence (Senmayo gene-set) AUCell scores, showing cell-type and group differences (E) and global distribution (F).

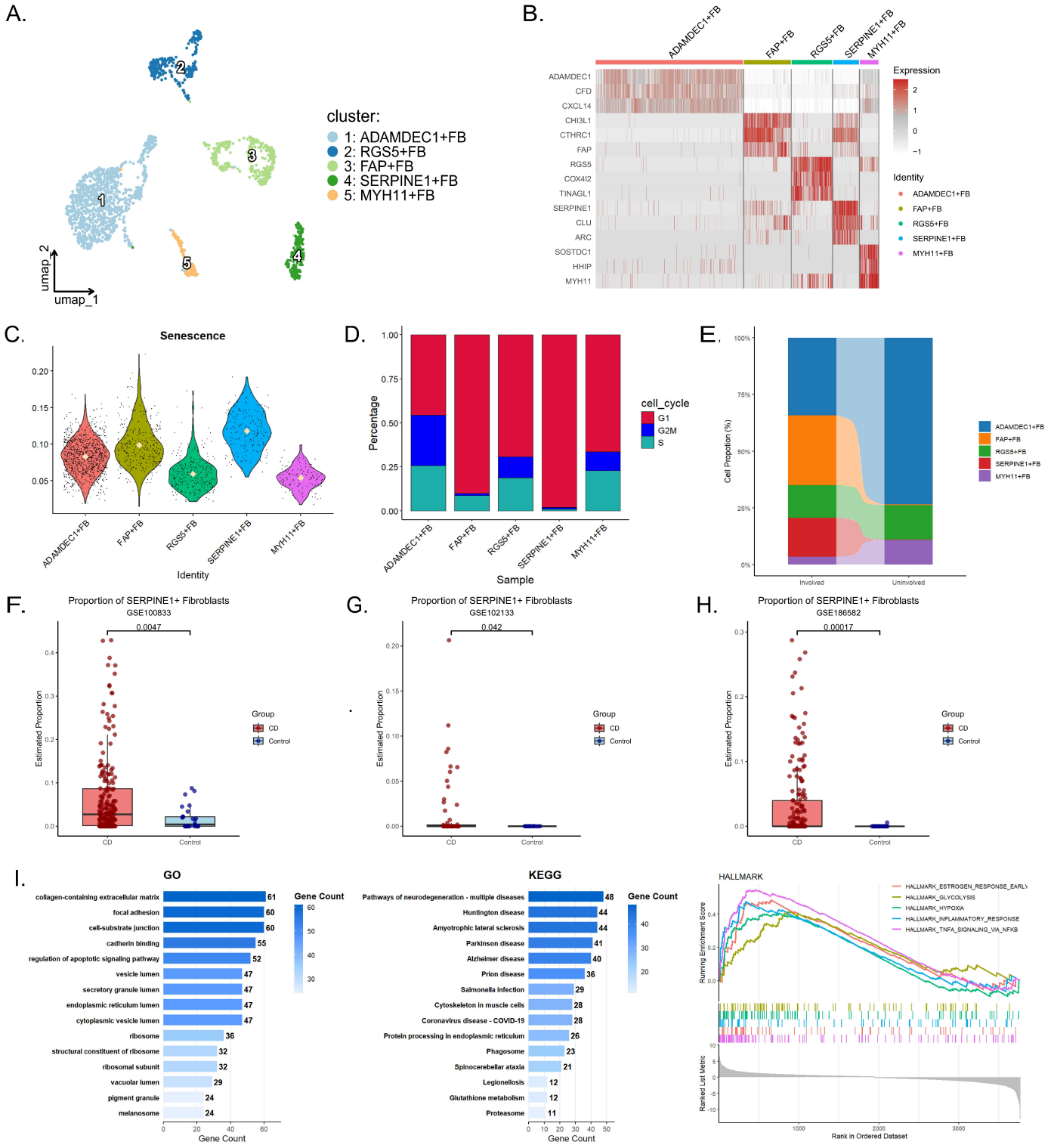


Figure 2

SERPINE1⁺ fibroblasts represent inflammation- specific senescent cells driving disease pathogenesis. (A) UMAP plots of the subclustered fibroblasts. (B) Heatmap of discriminative marker genes used to

define fibroblast subclusters. (C) Violin plot of Senmayo (senescence) AUCell scores across fibroblast subpopulations. (D) Stacked bar chart of cell-cycle phase distributions across fibroblast subclusters. (E) Stacked bar plot showing proportional abundance of fibroblast subclusters between involved and uninvolved groups. (F-H) Box plots of CIBERSORTx-deconvolved SERPINE1+ fibroblast proportions in three independent GEO datasets (GSE100833, GSE102133, GSE186582), comparing Crohn's disease (CD) versus control tissue. (I) GO, KEGG and GSEA enrichment results for the SERPINE1+ fibroblast gene set.

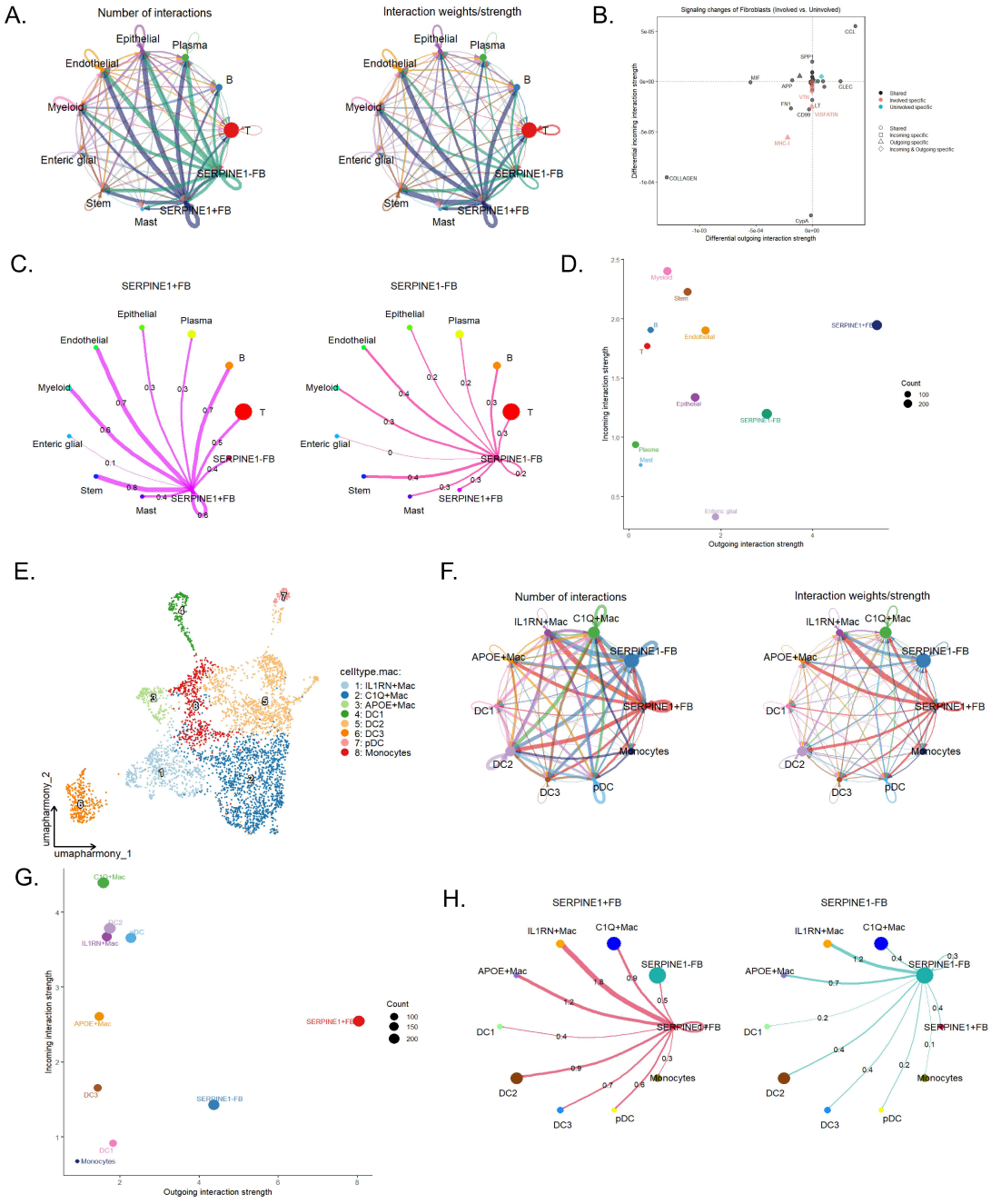


Figure 3

SERPINE1+ Fibroblasts Function as Communication Hubs in Crohn's Disease. (A) CellChat circle plot of global intercellular communication networks. (B) Differential cell-cell communication strength between involved and uninvolved fibroblasts. (C) Circle plot comparing inter-cell-type communication strengths between SERPINE1+ and SERPINE1− fibroblasts. (D) Dotplot of total outgoing and incoming signaling strength for each cell population, highlighting SERPINE1+ fibroblasts among the top communicators. (E) UMAP visualization of myeloid cell sub-clusters after re-clustering and annotation. (F) Circle plot summarizing global cell–cell communication between myeloid subsets and fibroblast subpopulations. (G) Dot plot comparing outgoing and incoming signaling strength among myeloid and fibroblast subpopulations. (H) Circle plot comparing communication strength between SERPINE1+ versus SERPINE1− fibroblasts and individual myeloid subpopulations.

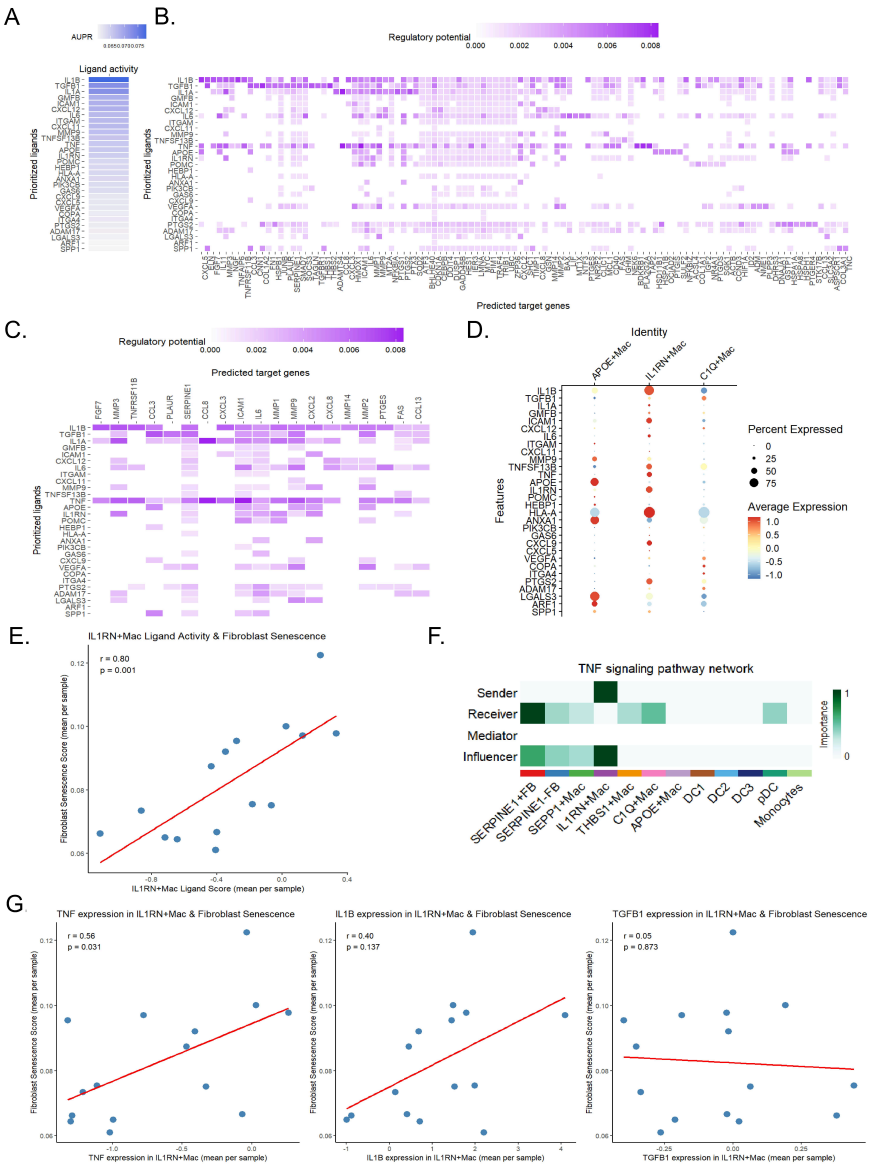


Figure 4

IL1RN+ Macrophages Drive Fibroblasts Senescence via TNF-α Signaling.(A-B) Heatmap showing the activity of ligands inferred to regulate SERPINE1+ fibroblasts by myeloid subsets (A), the predicted downstream target genes within SERPINE1+ fibroblasts (B). (C) Heatmap of ligand activities and their predicted senescence-associated target genes in fibroblasts, ranked by regulatory potential. (D) Dot plot showing expression (size = percent expressed; color = mean level) of key ligands across myeloid sub-

populations. (E) Scatterplot showing the positive correlation between IL1RN+ macrophage ligand activity and fibroblast senescence score across samples (r = 0.80, p = 0.001). (F) Heatmap of the TNF signaling pathway highlighting the main sender and receiver cell populations inferred by CellChat. (G) Scatterplots showing correlations between IL1RN+ macrophage expression of TNF, IL1B and TGFB1 (x-axis) and fibroblast senescence score (y-axis); TNF exhibits a significant positive correlation (r = 0.56, p = 0.031), whereas IL1B and TGFB1 show no significant association.

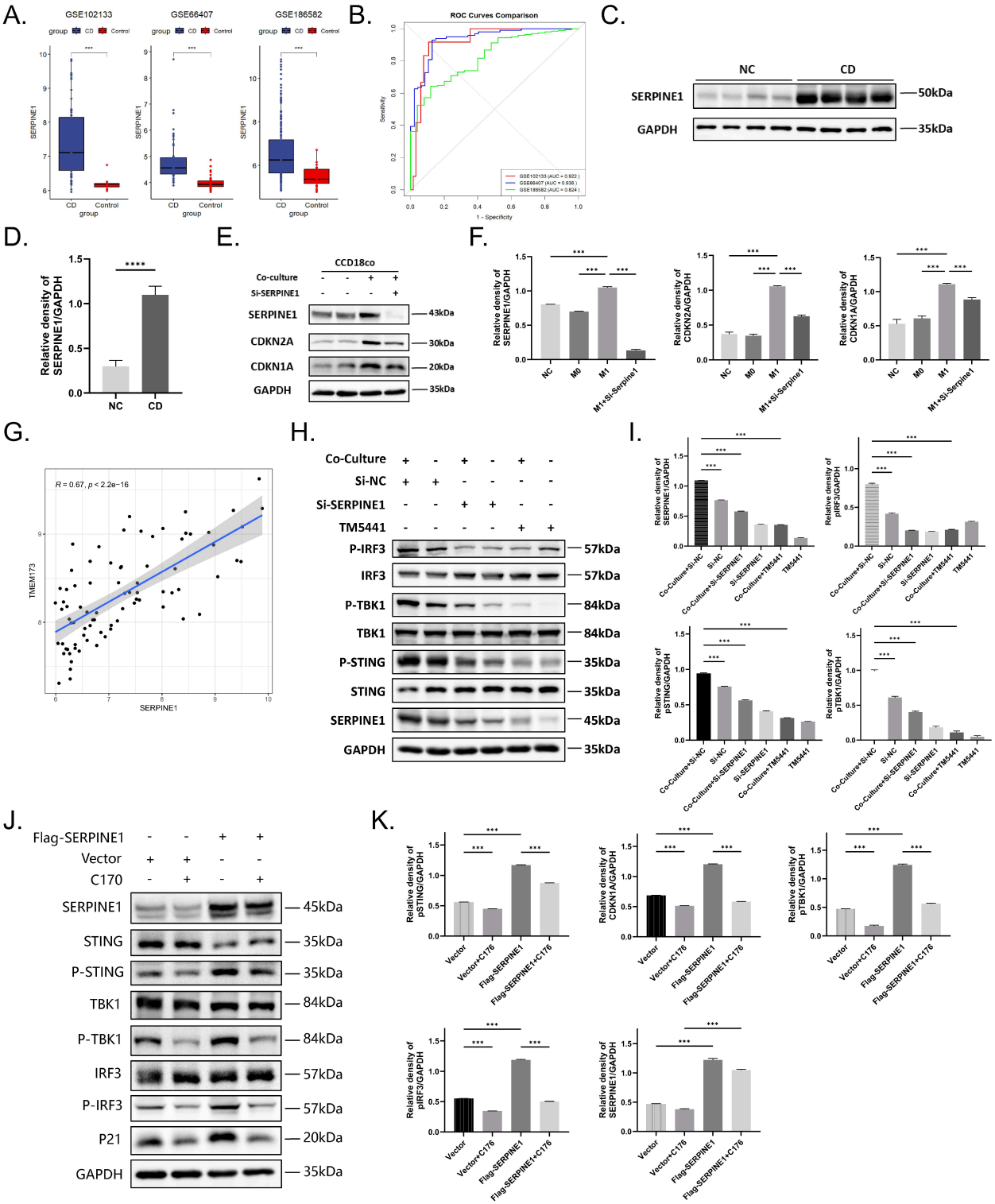


Figure 5

SERPINE1 drives cGAS-STING-mediated cellular senescence and pro-inflammatory signaling in Crohn's disease (A) SERPINE1 expression is significantly elevated in CD patients across three public datasets. (B) SERPINE1 shows strong diagnostic performance (AUC > 0.8) across three datasets. (C-D) Elevated SERPINE1 protein expression in human intestinal tissues from CD. (E-F) SERPINE1 knockdown suppresses M1 macrophage-fibroblast co-culture-induced inflammatory SASP expression. (G) correlation between SERPINE1 and TMEM173 (STING) expression in Crohn's disease (GSE75214). Pearson correlation coefficient $R = 0.67$, $p < 2.2 \times 10^{-16}$. (H-I) SERPINE1 knockdown and pharmacological inhibition attenuate cGAS-STING pathway activation. (J-K) SERPINE1 overexpression promotes cGAS-STING pathway activation, and STING inhibition rescues SERPINE1-induced senescence.

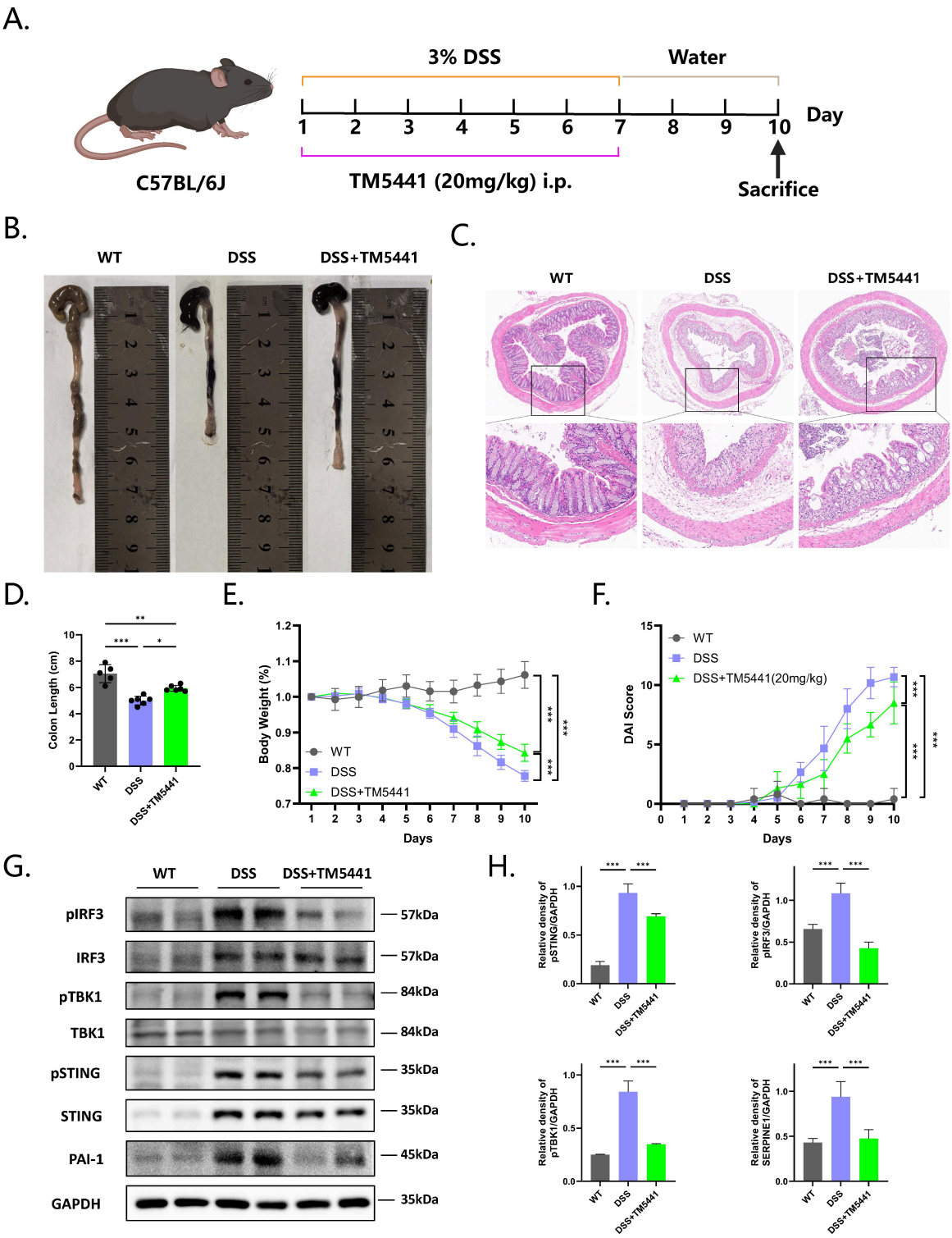


Figure 6

Validating Serpine1 as a DSS therapeutic target using TM5441 (A) Schematic overview of the experimental design using the selective SERPINE1 inhibitor TM5441 in the DSS-induced mouse model. (B) Representative photographs of colons. (C) H&E staining of colon sections. Scale bar: 200 μm (or 50 μm for enlarged regions). (D) Quantification of colon length. (E) Body weight trajectories demonstrate

that TM5441 treatment significantly attenuates DSS-induced weight loss.(F) Disease activity index (DAI) score. (G) TM5441 significantly inhibits STING pathway activation in DSS-treated mice.

Supplementary Files

This is a list of supplementary files associated with this preprint. Click to download.

- Supplimentaryfigure.docx
- Supplimentarytable1.docx
- Supplimentaryfigure2.pdf
- Supplimentaryfigure1.pdf
- Supplimentaryfigure3.pdf
- RAWData.pdf